Bulletin of the Seismological Society of America. Vol. 64, No. 6, pp. 1919–1929. December 1974

INTERPRETATION OF BODY AND RAYLEIGH WAVES FROM NTS TO TUCSON

BY CHARLES A. LANGSTON AND DONALD V. HELMBERGER

ABSTRACT

A linear array of eight Caltech portable broad-band seismograph trailers was set out from NTS to near Phoenix, Arizona, for the pre-announced underground nuclear test, OSCURO, on September 21, 1972. Travel-time and amplitude information were used to find an average crustal model by calculating synthetic seismograms using the Cagniard-de Hoop method. Rayleigh waves from other nuclear events at NTS, as recorded at the Tucson WWSSN station, were examined as a control for determining the structure of the top half of the crust. Group-velocity curves were found and synthetic Rayleigh waves calculated for Tucson and Kingman (LRSM). The formations and characteristics of P_n, a reflected P_n, and the P_g phases are examined. P_g is demonstrated to be composed of the primary P reflection from the mantle and contains multiple arrivals of P—SV conversions. Comparisons of synthetic and observed seismograms indicate a crustal thickness of 30 km with a Poisson's ratio of 0.23. The crust-mantle transition appears to be sharp, jumping from 6.1 to 7.9 km/sec. The amplitude behavior of P_n shows little evidence of any lid structure.

INTRODUCTION

In previous years determination of crustal structure through long-range refraction lines has been largely limited to the techniques of travel-time analysis and qualitative observations of amplitude information. Many crustal models found from these methods have been published and have been very useful in determining the broad characteristics of the Earth's crust and tectonic development. It was the hope of many investigators, however, that these studies could be checked by constructing synthetic seismograms and comparing these with the observations. In this way, interpretations could be verified and further refinements made in the model.

In this paper, a refraction line from NTS running into mid-Arizona is studied. Previous refraction work by Diment *et al.* (1961) was done along the same profile and serves both as a starting point in this study and as a supplement to our interpretations.

Using the Cagniard-de Hoop method of calculating synthetic seismograms (Helmberger, 1968), synthetics were fitted to the observed refraction records in an effort to determine the crustal structure more accurately than previously done. In addition, Rayleigh waves were examined from previous nuclear explosions at NTS as recorded at the WWSSN station at Tucson along the same line. Dispersion curves for several intermediate explosions were obtained and two synthetic records calculated using the Thompson-Haskell layer-matrix technique as developed by Harkrider (1964). These two techniques of using body waves and Rayleigh waves were played against each other in an effort to constrain the crustal model.

Another primary goal of this study is to examine and explain the P_g phase. The Cagniard-de Hoop method proved to be well suited for such an interpretation.

Data Reduction

An array of eight Caltech portable seismograph trailers was set out along a southeast-trending line from NTS to Luke AFB, Arizona, for the preannounced underground nuclear test, OSCURO, which occurred on September 21, 1972 (Figure 1). The line was in the southeastern part of the Basin and Range province and follows regional topographic and structural trends. Previous refraction work, by Diment *et al.* (1961), has been done along the northwest half of the present line from NTS to Kingman, Arizona.

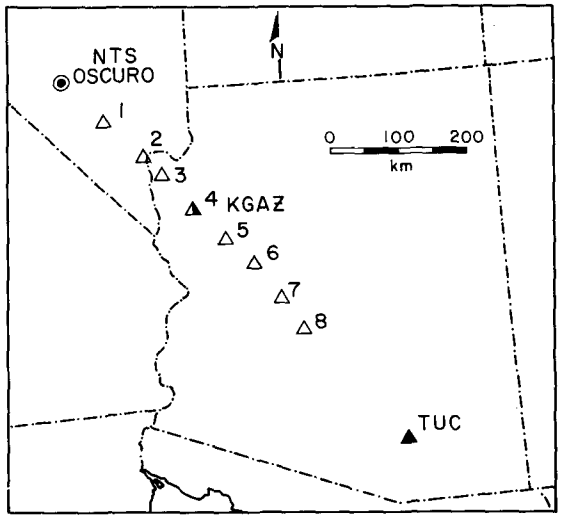

FIG. 1. Index map of the stations used in this study. Open triangles show the location of the trailer array; half-open triangle, combined location of trailer and an LRSM station; solid triangle, WWSSN station.

TABLE 1

STATION LOCATIONS AND TRAVEL-TIME CORRECTIONS

Station No.	Name	Latitude	Longitude	Distance From Source (km)	Elevation (meter)	Travel-Time Correction
1	Corn Creek	36°26.32′	115°21.55′	92.91	890	−.16
2	Boulder City	35°58.71′	114°50.45′	162.1	768	−.12
3	Charlie's Mine	35°42.27′	114°28.63′	207.5	713	+.18
4	Kingman	35°11.92′	114°02.41′	276.1	1140	+.11
5	Seapy's Ranch	34°46.38′	113°36.43′	337.9	640	+.19
6	Gibson's Canyon	34°26.21′	113°06.84′	395.6	658	+.19
7	Wickenburg	33°59.46′	112°40.85′	458.6	768	+.17
8	Luke AFB	33°32.35′	112°20.48′	516.5	335	+.02

Data from the blast are displayed in Figures 2 and 3. Two distinct phases are seen, P_n and P_g, having apparent velocities of 7.9 and 6.1 km/sec, respectively. Also, there is a hint of another phase, designated P_n', coming in after P_n and before P_g for the three farthest stations with an apparent velocity comparable to P_n. More will be said about these phases later.

First-order station corrections for elevation and geology were calculated by first consulting geological and topographic maps. Using a datum of 700 meters and assuming

the crystalline rocks have a compressional velocity of 5.9 km/sec and sediments, 3.0 km/sec, travel-time corrections were no greater than 0.2 sec (Table 1). The data were read to accuracies of 0.2 sec for P_n and 0.5 sec for P_g and P_n'. The travel times were then fitted with a least-squares line to find the apparent velocities. Ranges were calculated by computer using the geographical coordinates of the source and receivers. Figure 4 shows the resulting travel-time curves.

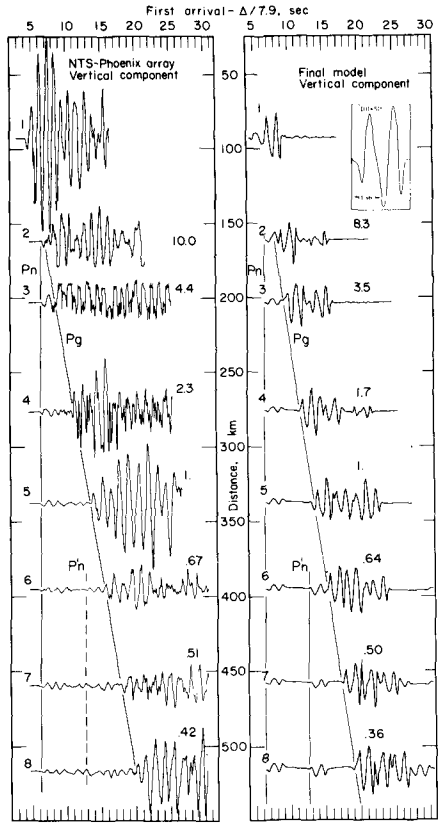

FIG. 2. Observed and synthetic seismograms. *Left-hand portion* displays observed vertical component of trailer array. *Right-hand side* shows the final synthetics calculated from model B. The wave form in the *upper right-hand corner* is the $I(t) * S(t)$ used in all the synthetic seismogram calculations. Travel-time lines have been drawn in for the P_g, P_n, P_n' phases. Station numbers are to the left of each seismogram and relative zero to peak amplitudes are to the right.

DATA INVERSION

Essentially, the method of data inversion used in this paper is the following. Using the travel times, a simple layered earth model can be made provided the interpretations of the observed phases are correct. This serves as a starting model for the calculation of synthetic seismograms. The amplitude behavior of the synthetics is examined and compared to the data and a further iteration performed on the model until a satisfactory match is obtained.

BODY WAVES

Body-wave synthetic seismograms were computed by the Cagniard-de Hoop method. The object was to fit the first 10 to 25 sec (the P_n and P_g phases) of the observations as closely as possible.

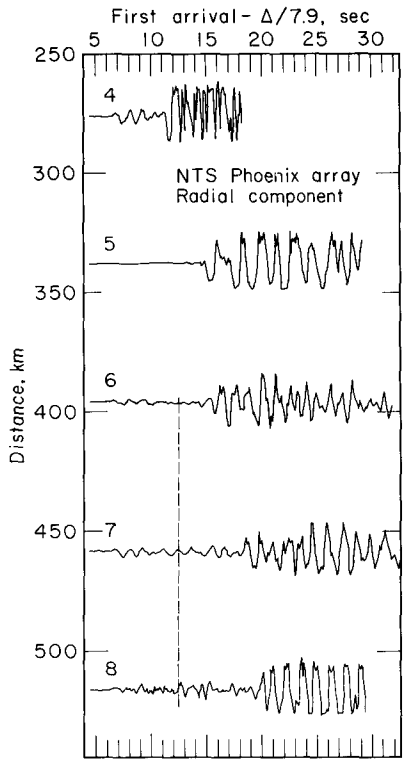

FIG. 3. Observed radial components. Dotted line shows interpreted arrival of the P_n' phase.

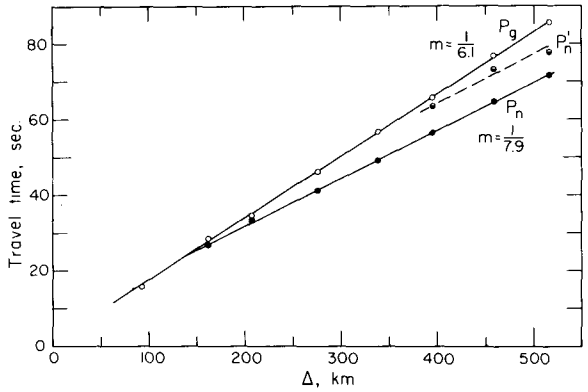

FIG. 4. Least-squares fit to P_n and P_g travel times. Dotted line for P_n' is inferred.

The first problem encountered in calculating synthetics was finding a suitable source-time function. In dealing with linear elastic-wave theory, the seismogram can be decomposed into several parts as the following equation illustrates

$$S_R(t) = M(t) * I(t) * S(t)$$

where $S_R(t)$ is the trace of the seismogram; $M(t)$, the impulse response of the layered earth structure; $I(t)$, the impulse response of the instrument; $S(t)$, the effective point source-time function; and $*$, the convolution operator. $S(t)$ was not known so the following approximate method was used. We suppose that a simple head wave acts as the time

integral of the direct wave or source history. One can then take the P_n phase off the seismogram, differentiate it, and obtain $I(t) * S(t)$. This was done using station 5. In the upper right-hand corner of Figure 2 the pulse used in all the body-wave synthetic seismogram calculations is displayed. Included in the $S(t)$ is the interaction with the free surface, such as pP, and any contributions from fine structure near the surface. We will assume that $S(t)$ is invariant over the small range in ray parameters considered.

The first crustal model computed was Diment's *et al.* (1961) proposed model (their Figure 8) as shown in Table 3. Figure 5(a) shows the synthetic seismograms obtained. The synthetics disagree with the observations mainly because of the 8.1-km/sec layer

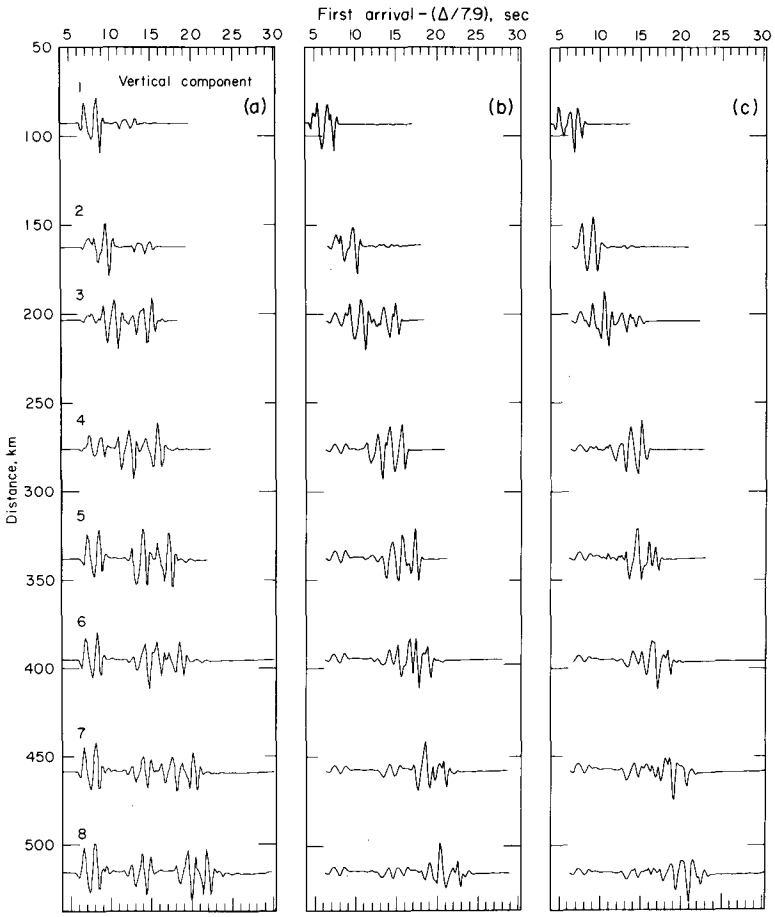

FIG. 5. Profile (a) contains synthetics assuming the model given by Diment *et al.* (1961) as given in Table 3. Profile (b) contains synthetics assuming a modified model A with a 5-km intermediate layer. Profile (c) contains synthetics for a model similar to (b) but with a 10-km intermediate layer.

which caused a large reflection to come in at the onset. The amplitude of this reflection (looking at stations 4 to 8) is comparable to the rest of the record. The third pulse in seismogram 8 starts with the reflection from the 6.15 to 7.81-km/sec interface, which is comparable in travel time to the P_g phase in the observation. Taking out the 8.1-km/sec layer produces synthetics which compare fairly well in relative amplitudes of both P_n and P_g but are off a few seconds in travel time because of the different velocities observed in this study.

Before a better model was attempted, however, it was realized that this profile was deficient in resolving the structure of the upper half of the crust. Diment *et al.* (1961) found that for close-in distances to NTS the crust predominately yielded velocities of 6.15 km/sec. Because this gave a localized velocity structure, it was felt that it may not be applicable to the entire profile. To get an idea of how the upper part of the crust acted, on the average, Rayleigh waves from NTS events as recorded at the WWSSN station at Tucson were analyzed. Tucson was ideal since it lay on the same line as the profile.

Rayleigh Waves

Nine low-intermediate events were examined (Table 2). A typical record is displayed in the *lower half* of Figure 6. Group velocity curves for the nine events were determined by the peak-and-trough method. This assumes that there is no group delay at the source, with relatively small amplitude variations on the record, and that the wave is well dispersed. The assumption of small amplitude variations seems to be the weakest but will be tested by constructing a synthetic Rayleigh wave.

Peaks and troughs were counted, using the digitizer, and plotted versus travel time. A cubic was fitted through each data set by least-squares, analytically differentiated to

TABLE 2

NTS Event Locations

Name	Date	Time	Latitude	Longitude	Δ (NTS–TUC) (km)
OSCURO	9/21/72	15:30:00.2	37.082°N	116.037°W	
CHARTREUSE	5/6/66	15:00:00.1	37.35°	116.32°	754.3
COMMODORE	5/20/67	15:00:00.2	37.13°	116.06°	720.7
BOURBON	1/20/67	17:40:04.4	37.10°	116.00°	714.6
DUMONT	5/19/66	13:56:28.1	37.11°	116.06°	719.1
DURYEA	4/14/66	14:13:43.1	37.24°	116.43°	752.4
BRONZE	7/23/65	17:00:00.0	37.10°	116.03°	716.4
BUFF	12/16/65	19:15:00.0	37.07°	116.03°	714.0
PILEDRIVER	6/2/66	15:30:00.1	37.23°	116.06°	728.8
CORDUROY	12/3/65	15:13:02.1	37.16°	116.05°	722.5
BOXCAR	4/26/68	15:00:01.1	37.29°	116.46°	293 to KGAZ

find the period arrival-time curve, and then, using the calculated distance, the group-velocity dispersion curve was determined. The curves for the nine events were nested together and an "average" curve drawn between the extremes. The accuracy of the final averaged curve is taken to be the spread in the nested curves. Figure 7 shows the obtained dispersion curves.

Inversion of the averaged curve was done by trial and error. Using the Thompson-Haskel layer matrix method as developed by Harkrider (1964), dispersion curves were calculated from various models. The body-wave data were used as a constraint for the lower part of the crust because the Rayleigh waves were only sampling approximately the upper 20 km. An attempt was made to hold Poisson's ratio at 0.25 so that the shear velocity would determine the compressional velocity. The velocity constraints on the models, however, required that the shear velocity vary somewhat independently of the compressional velocity. This ultimately produced a Poisson's ratio of 0.23 for the main part of the crust in the final models.

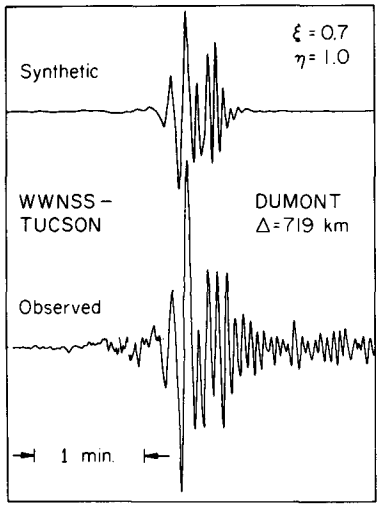

FIG. 6. Observed and synthetic Rayleigh waves for the Tucson WWSSN station. *Lower half* shows a typical Rayleigh wave from events at NTS. *Upper half* is a synthetic Rayleigh wave calculated using model B. The source parameters used are displayed in the *upper right-hand corner.*

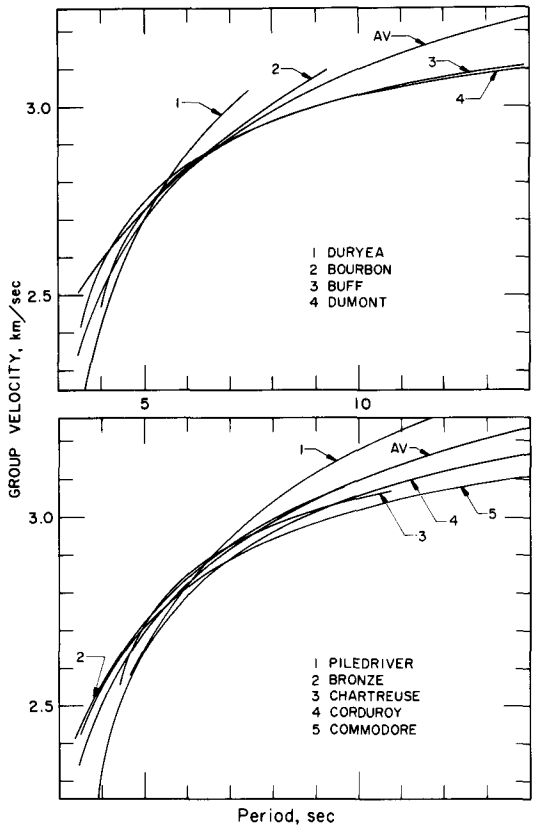

FIG. 7. Nested group-velocity dispersion curves obtained from events at NTS.

MODELS

The models obtained are displayed in Table 3. Two models were found to fit the Rayleigh- and body-wave data equally well. Model A is most like the Diment *et al.* (1961) model with the major differences being in velocity and overall thickness. The second and third layers of model B should be interpreted as an increasing velocity gradient as seen by the Rayleigh waves and not as discrete layering.

TABLE 3

PROPOSED CRUSTAL MODEL PARAMETERS

Model	Layer	Thickness (km)	*P* velocity (km/sec)	*S* velocity* (km/sec)	Density* (gm/cm³)
Diment, Stewart, Roller (1961) (taken from their Figure 8)	1	1.7	3.0	1.7	2.3
	2	28.4	6.15	3.55	2.8
	3	24.4	7.81	4.5	3.2
	4	—	8.1	4.7	3.3
A	1	1.0	3.0	1.73	2.3
	2	31.0	6.1	3.6	2.8
	3	—	7.9	4.6	3.2
B	1	1.0	3.0	1.73	2.3
	2	1.0	5.5	3.3	2.5
	3	2.0	5.9	3.4	2.7
	4	25.5	6.1	3.6	2.8
	5	—	7.9	4.6	3.2

* *S* velocity and density used in calculations of synthetics not given by Diment *et al.* (1961).

The most important aspect of these two models is that lower-velocity materials in the upper portion of the crust are thin and that the crust largely behaves like one 6.1 km/sec layer. Both models explain the data equally well and both are just as plausible. If any preferred model is to be taken, it should be model A, just because of its simplicity.

RAYLEIGH WAVES

A Rayleigh-wave synthetic seismogram was calculated for the event DUMONT. The time-source function (Helmberger and Harkrider, 1972).

$$S(t) = t^{\xi}e^{-\eta t}$$

was used, where the parameters ξ and η were found by trial and error to be 0.7 and 1.0, respectively. The fit (Figure 6) is remarkable considering the assumptions made in the analysis. Group arrivals are in complete agreement and relative amplitudes are good. The seismograms of Figure 6 have not been normalized to each other.

As a test of the model closer to NTS, the event BOXCAR, as recorded at the LRSM station KGAZ, Kingman, Arizona, was used. Source parameters were obtained for this event by Helmberger and Harkrider (1972). The synthetic obtained (Figure 8) is in good agreement with respect to group arrivals and relative amplitudes but had to be shifted 4 sec back in time to line up with the observation. This is a discrepancy of about 0.1 km/sec in overall group velocity and indicates that the crust may have slightly smaller velocities in the northwest portion of the profile.

Body Waves

Body-wave synthetics were calculated for model B and are displayed in Figure 2. The travel times and relative amplitudes fit well and even wave shapes are good in some cases. The observed records have not been normalized. The synthetics are normalized with respect to maximum amplitudes attained by each. The good agreement of P_n wave shapes, especially at station 5, is an indication that the assumption of $I(t) * S(t)$ was good in the calculations.

Discussion

Through the examination of the amplitude behavior of the synthetics a few points about the fine structure of the crust and propagation effects can be made.

Perhaps the most interesting and obvious point to be made from these synthetics concerns the formation of the P_g phase. The calculated P_g phase, as defined in this profile, includes the primary reflection from the M-discontinuity as the first arrival with the first crustal multiple arriving a few seconds afterward and contributing almost as much energy. Also included are rays which traverse one leg as SV waves. The most important conversions are those associated with the surface layer, which contribute perhaps 10 per cent of the energy in the calculated P_g phase. Obviously, at some stations, the synthetics do not match the observations in peak amplitudes. This deficiency is interpreted as a lack of including near-surface (upper 5 km) ringing effects or multiple rays

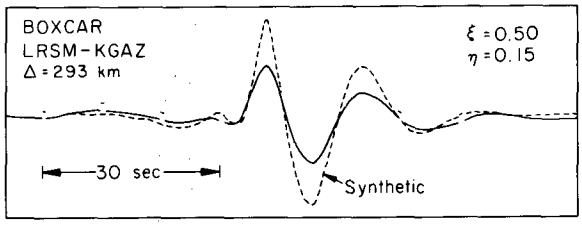

FIG. 8. Synthetic and observed Rayleigh waves from BOXCAR for KGAZ. Synthetic calculated from model B. Source parameters for the synthetic are displayed in the *upper right*.

which occur in the upper layers. This effect will be strongly dependent on local geology and, hence, cannot be modeled adequately by the techniques used here.

The crustal wave-guide explanation as deduced by others, for example, Press and Gutenberg (1956) and Shurbet (1960), seems to be fundamentally correct. However, there is still a problem in determining just what are the wave-guide boundaries. In this profile, the entire crust behaves largely as one layer with compressional-wave velocity of 6.1 km/sec. The corresponding P_g phase observed here is slightly faster than the 5.9-km/sec apparent velocity more commonly observed, due to having the wave guide composed of the M discontinuity and the free surface. Other crustal structures will change the character of the phase. For instance, in an area with an intermediate layer, such as the so-called Conrad discontinuity, the P_g phase will be complicated through the interaction of the M discontinuity and the intermediate boundary. Another modeling study, similar to this one, for mid-continent crust would be needed to resolve the problem.

As shown in Figure 2 the relative amplitude behavior of P_n, between observations and synthetics, is remarkably good. This suggests that the upper mantle under the profile is free from any significant velocity gradients, both positive and negative. Synthetic models were run for gradients of approximately 0.02 sec^{-1}. The synthetics obtained were significantly different in amplitudes as compared with the observations. A positive

gradient boosted up the amplitude of P_n to values approaching the size of P_g. The negative gradient had a less drastic effect but a significant variation in apparent travel time and wave shape was observed. The conclusion is, based on the data and synthetics, that any velocity gradients in the uppermost mantle must be much less than 0.02 sec^{-1}, probably lower than 0.005 sec^{-1}, and cannot be distinguished with these observations.

The P_n' phase, as designated here, is emphasized to be only a possible interpretation. This phase is a head wave associated with the first crustal multiple. Evidence for it is slight and can be seen in Figures 2 and 3. The strongest indications of its existence are the interference effect of P_n coming out of the P_g phase, which is clear in the final synthetics and suggestive in the observations (Figure 2), and the prominent arrival at station 8 (Figure 3). The lack of coherence of this low-amplitude phase may not be surprising, considering that part of its path consists of a surface reflection where the local geology is very important. Reverberation near the receiver in the upper layers for P_n may also be important.

Conclusions

Two average crustal models are presented for a profile from NTS to Phoenix, Arizona, which differ somewhat from those given by Diment *et al.* (1961). It is shown that an 8.1-km/sec layer, 53 km below the surface, does not exist. The uppermost mantle has an average compressional velocity of 7.9 km/sec and has no observable velocity gradients from the study of P_n amplitudes. The crust is 30 km and acts largely as one 6.1-km/sec layer. The models presented differ in that one has an increasing velocity gradient from 5.5 to 6.1 km/sec over 3 km at the top, whereas the other preferred model, which is similar to Diment's *et al.* (1961), consists of one 28.9-km-thick, 6.1-km/sec layer.

The absence of an intermediate-velocity crustal layer in this profile is remarkable and deserves comment on the resolvability of detecting it. The present refraction profile starts at 93 km so one could argue that the 6.8-km/sec branch of a travel-time curve is obscured by the M discontinuity head wave and reflection. However, Diment *et al.* (1961) observed no crustal velocities higher than 6.15 km/sec out to P_n distance.

Test models were run to see if, by using the technique described, one could resolve a layer of 6.8 km/sec material. Figure 5, (b) and (c) show the synthetics. Figure 5(b) is based on a crustal model the same as model A but with a 25-km, 6.1-km/sec upper crust and a 5-km, 6.8-km/sec lower crust. Figure 5(c) is based in a 21.4-km, 6.1-km/sec upper crust and a 10-km, 6.8-km/sec lower crust. In both models, P_g arrives early. Comparison of the wave shapes at station 2 (Figure 2) with the synthetics of Figure 2 and Figure 5, (b) and (c), indicates that the model consisting of a 10-km, 6.8-km/sec layer fits the poorest with the 5-km layer model fitting better. The model with no intermediate layer fits the best (Figure 2) in terms of the separation of the first two positive peaks. It is concluded, therefore, that there is no clear intermediate layer along this profile on the basis of the previous observations and model studies presented here.

A shear-velocity profile obtained by Rayleigh-wave analysis, taken with the compressional-wave profile, yields a Poisson's ratio of approximately 0.23 for the crust.

Synthetic seismograms were calculated for both Rayleigh waves and body waves and agree very well with the observations. Calculation of a Rayleigh-wave synthetic for the BOXCAR event for the northwest portion of the profile indicates that the crust may have slower velocities, perhaps up to 0.1 km/sec less than those obtained over the entire profile.

The P_g phase has been experimentally verified, along this profile, as consisting mostly of the primary reflection off the Moho followed by crustal multiples. Rays with one leg

of SV energy also contribute to the phase. The P_g phase in more complicated crustal structures will be more complicated due to the increasing number of boundaries in the crustal wave guide.

Acknowledgments

We thank David Harkrider for the use of his programs and advice. This reasearch was supported by the Advanced Research Projects Agency at the Department of Defense and was monitored by the Air Force Office of Scientific Research under Contract F44620-72-C-0078.

References

Diment, W. H., S. W. Stewart, and J. C. Roller (1961). Crustal structure from the Nevada Test Site to Kingman, Arizona, from seismic and gravity observations. *J. Geophys. Res.* **66,** 201–214.

Harkrider, D. G. (1964). Surface waves in multilayered elastic media, 1. Rayleigh and Love waves from buried sources in a multilayered elastic half-space, *Bull. Seism. Soc. Am.* **54,** 627–679.

Helmberger, D. V. (1968). The crust-mantle transition in the Bering Sea, *Bull. Seism. Soc. Am.* **52,** 299–319.

Helmberger, D. V. and D. G. Harkrider (1972). Seismic source descriptions of underground explosions and a depth discriminate, *Geophys. J.* **31,** 45–66.

Press, F. and B. Gutenberg (1956). Channel P waves, Πg, in the earth's crust, *Trans. Am. Geophys. Union,* **37,** 754–756.

Shurbet, D. H. (1960). The P phase transmitted by crustal rock to intermediate distances, *J. Geophys. Res.* **65,** 1809–1814.

Division of Geological and Planetary Sciences
California Institute of Technology
Pasadena, California 91109
Contribution No. 2451

Manuscript received February 11, 1974